



Experimental Measurements of Viscosity and Thermal Conductivity of Single Layer Graphene Based DI-water Nanofluid

Prof. Dr. Najdat N. Abdulla

Department of Mechanical Engineering
University of Baghdad
E mail: najdat_abdulla@yahoo.co.uk

Hussein A. Ibrahim

Department of Mechanical Engineering
University of Baghdad
E mail: hussain1983ali@gmail.com

ABSTRACT

Experimental measurements of viscosity and thermal conductivity of single layer of graphene based DI-water nanofluid are performed as a function of concentrations (0.1-1wt%) and temperatures between (5 to 35°C). The result reveals that the thermal conductivity of GNPs nanofluids was increased with increasing the nanoparticle weight fraction concentration and temperature, while the maximum enhancement was about 22% for concentration of 1 wt.% at 35°C. These experimental results were compared with some theoretical models and a good agreement between Nan's model and the experimental results was observed. The viscosity of the graphene nanofluid displays Newtonian and Non-Newtonian behaviors with respect to nanoparticles concentration and temperature, and about 111% enhancement was obtained compared to the base fluid with GNPs weight fraction concentration of 1wt.% at 35°C. Based on the experimental data, correlations were developed for predicting thermophysical properties of the GNPs based DI-water nanofluid.

Key words: Graphene, Nanofluid, Thermal conductivity, Viscosity, Experimental measurements

القياسات التجريبية للموصلية الحرارية واللزوجة لمائع نانوي احادي الطبقة (كرافين - ماء)

حسين علاوي ابراهيم
قسم الهندسة الميكانيكية
جامعة بغداد

أ.د. نجدت نشأت عبدالله
قسم الهندسة الميكانيكية
جامعة بغداد

الخلاصة

قياسات اللزوجة والموصلية الحرارية للمائع النانوي احادي الطبقة (كرافين- ماء) اجريت وفقا لكل من التراكيز 0.1-1wt% ودرجة حرارة (5 to 35°C). اظهرت النتائج ان الموصلية الحرارية للمائع النانوي (كرافين- ماء) تزداد بزيادة تركيز الجزيئات النانوية للكرافين ودرجة حرارة المائع وكان الحد الأقصى للتعزيز حوالي 22% لتركيز (1 wt %) في (35°C).

هذه النتائج التجريبية قورنت مع بعض النماذج النظرية ورصد اتفاق جيد بين نموذج نان والنتائج التجريبية. اللزوجة للمائع النانوي (كرافين- ماء) يبدي سلوك نيوتيني وغير نيوتيني اعتمادا على تركيز الجزيئات النانوية ودرجة الحرارة، ونحو



11% زيادة مقارنة مع السائل الأساسي مع تركيز (1 wt %) ودرجة حرارة 35°C. استنادا إلى البيانات التجريبية، تم إيجاد علاقات ترابطية للتنبؤ بالخصائص الحرارية للمائع النانوي كرافين-ماء. الكلمات الرئيسية: كرافين، مائع نانوي، الموصلية الحرارية، اللزوجة، القياسات العملية.

1. INTRODUCTION

Most heat transfer applications use conventional fluids like ethylene glycol (EG), DI-water and engine oil as heat transfer working fluids. The efficiency of these fluids is often limited by their low heat transfer capacities so the efficiency of the conventional fluids can be enhanced by improving the heat transfer properties and thermal conductivity. These heat transfer fluids have low thermal conductivity with respect to solid materials. Therefore, solid particles with high thermal conductivity are generally added to traditional heat transfer fluids to increase their thermal conductivity. However, the addition of micrometer or millimeter particles sized can cause problems as sedimentation and agglomeration. **Choi, 1995**, avoided these problems by introducing a new kind of heat transfer medium referred to nanofluid where the nanoparticles size less than (100 nm) are dispersed in base fluids like EG, water and oil.

The benefits of nanofluids technologies are expected to be large due to the heat transfer characteristic of cooling devices or heat exchangers in many applications. For example, the thermal transport industry requires minimizing the weight and size of thermal systems of vehicles and nanofluids can enhance thermal transport of lubricants and coolants. The nanoparticles when properly dispersed in base fluid, nanofluids can show many advantages besides the abnormal high effective thermal conductivity. These advantages involve, reduction in pumping power, improving heat transfer and stability, miniaturizing systems, micro channel cooling without clogging and savings cost and energy **Murshed, 2008**.

Many different nanoparticale materials are used for preparation nanofluids, such as metals (Cu, Al, Au, Fe and Ag), metal oxide (CuO, Al₂O₃, MgO), carbide ceramics (SiC, TiC), Semiconductors (SiO₂, TiO₂) and Carbon nanostructures as (graphite, diamond, carbon nanotube, graphene, graphene oxide). Carbon nanostructures materials are utilized due to their extremely high thermal conductivity (k) in the axial directions, low density and large surface area compared with metals or metal oxides materials.

Base fluids mostly used in the producing of nanofluid are the conventional fluid such as ethylene glycol, water and oil.



Recently, several investigations were devoted to study the thermal properties such as viscosity and thermal conductivity of the nanoparticles based nanofluid prepared from different carbonic structures, like single-wall, multiwall carbon nanotubes, graphite nanoparticles, and diamond nanoparticles, graphene oxide, graphene. Among all of these structural forms, single layer graphene is a 2-D material with one carbon atom thickness layer was discovered by **Novoselov** in **2004**. It has unique thermal characteristics due to large specific surface area and high thermal conductivity compared with other carbonic forms. However, according to literature, experimental and theoretical studies on the heat transfer thermal properties like viscosity and thermal conductivity of graphene based nanofluids are scarce.

Ramaprabhu, 2010, carried out experimental study on thermal, electrical conductivities and heat transfer characteristics for hydrogen exfoliated graphene nanosheets dispersed in DI-water and EG-based nanofluids for different temperatures and volume fractions. The results of 0.05% volume concentration of hydrogen exfoliated graphene dispersed in DI-water based nanofluid was shown an improvement in thermal conductivity of around, 75%, 16% at 50°C and 25°C respectively.

Xie, 2011, investigated experimentally the thermal conductivity of graphene EG-based nanofluid. The result of 5.0% volume fraction of graphene dispersion showed significant improvement in the thermal conductivity of nanofluid up to 86%. The stiffness and 2D structure of graphene oxide and graphene helped to enhance the thermal conductivity of the nanofluids. The results of thermal conductivities of graphene oxide and graphene EG-based nanofluid were around ~4.9 and 6.8 W/m K, respectively.

Rashidi, 2013, studied the thermal conductivity and stability behavior of graphene based water nanofluid. The Thermal conductivity of graphene versus temperature and time for various weight concentrations were determined. Alkaline method was utilized to functionalize without any additives or surfactant. This method was successfully dispersed of graphene in water. Results suggested that there was an augmentation in thermal conductivity by increasing temperature and graphene weight fraction concentration. The best result showed augmentation of thermal conductivity about 14.1% with 0.05 wt.% of alkaline functionalized Graphene (AFG) with respect to water at 25 °C and 17% at 50 °C.

Dey, 2013, prepared a well dispersed and stable fictionalized graphene (f-HEG) base (distilled water and ethylene glycol) nanofluids with volume concentration between 0.041 to 0.395%.



Measurements of viscosity and thermal conductivity were performed at different volume concentrations and temperature between 10 to 70 °C. The results showed thermal conductivity enhancement about ~15% for a volume fraction of 0.395 vol.%. Viscosity of the nanofluids and base fluid showed non Newtonian behavior with the appearance of shear thinning and about 100% increment compared to the base fluid (ethylene glycol distilled water) with volume fraction of 0.395.%.

Rashidi, 2014, investigated the effects of graphene oxide (GO/water) nanofluid concentration and temperature on the thermal conductivity. Result indicated thermal conductivity of (GO/water) nanofluid higher than thermal conductivity of base fluid. Thermal conductivity depended strongly on the graphene oxide concentration and enhanced with increasing it. When the nanosheet weight fraction was 0.25wt.%, the enhancement ratio was 33.9% at 20°C and when the temperature increased up to 40°C the enhancement ratio up to 47.5%.

The aim of the present work is to measure experimentally viscosity and thermal conductivity of GNPs based DI-water nanofluid for various weight fraction concentrations and temperatures.

2. EXPERIMENTAL SET-UP

2.1 Viscosity Measurements

The viscosity of the GNPs based DI-water nanofluids at a different weight fractions concentrations (1, 0.9, 0.8, 0.7, 0.6, 0.5, 0.4, 0.3, 0.2 and 0.1wt%) were measured by using a rotational kind low viscosity DV-I prime digital model viscometer from (Laboratories of Brookfield Engineering Inc.) at convective heat transfer laboratory of Texas A&M University. The maximum torque rating for this model is 0.06737 m.N and a accuracy is $\pm 1\%$. The viscometer was calibrated by using a Brookfield's viscosity standard test fluid. **Fig. 1** shows the DV-I prime viscometer.

A combination of cylindrical spindle and sample container referred as UL adapter was utilized for taking measurements at low viscosity. This type of spindle can be used to measure viscosities of both non Newtonian and Newtonian fluids. The viscous drag experienced by the spindle in UL adapter was manufactory calibrated to offer percentage of maximum torque and dynamic viscosity by using Eqs. (1) and (2). on a digital output screen. **Operating Instructions Manual, 2014.**



$$\dot{\gamma} = \frac{2R_c^2}{(R_c^2 - R_{sp}^2)} \omega \quad (1)$$

$$\tau = \frac{M}{2\pi R_{sp}^2 L} \quad (2)$$

$$\mu = \frac{\tau}{\dot{\gamma}} \quad (3)$$

$$\omega = \frac{2\pi N}{60} \quad (4)$$

where R_c , R_{sp} , ω , M , L , μ , and N are radius of the sample container, radius of the spindle, angular speed of the spindle, torque input by the viscometer, effective length of the spindle, dynamic viscosity and rotational speed of the spindle, respectively as shown in **Fig. 2**.

Measurements are taken at different shear rates and temperatures range from (5, 10, 15, 20, 25, 30 and 35°C) and were repeated four times for each experiment to obtain accurate results.

The DV-I prime viscometer has been calibrated by using standard test fluid viscosity of (9.6cP) at temperature 25°C which provided by the Laboratories of Brookfield Engineering Inc. Its precision was found to be +/- 0.6%.

2.2 Thermal Conductivity Measurements

Thermal conductivity is one of the most effective parameters which has important effect on augmentation of heat transfer coefficient. Thermal conductivity of GNPs based DI-water nanofluids with six various weight fraction concentrations (1, 0.8, 0.6, 0.4, 0.2, 0.1 wt%) at temperatures range from (5-35°C) is measured by using a KD2 Pro instrument from (Decagon devices, Inc. USA). The measurements were taken under different temperature conditions by using a temperature-controlled container connected with chiller to maintain constant temperature of sample as shown in **Figs. 3** and **4**. These figures illustrate the experimental setup to measure thermal conductivity by using KD2 Pro instrument. The experimental set-up consists of: **1)** KD2 Pro microcontroller **2)** chiller **3)** probe needles **4)** temperature-controlled path.

The instrument working is based on the fundament of a transient hot wire method and has accuracy of about 5%. A KD2 Pro consists of a sensor probe needles and handheld microcontroller. The sensor probe needle is of stainless steel 60mm length and 1.3mm diameter and includes both a thermistor and a heating element. The controller module includes a microcontroller of 16-bit /AD converter, a power control circuitry, and battery.



The measurements of thermal conductivities are based on the following assumptions: (i) the medium is both isotropic and homogeneous (ii) the long source of heat can be considered as an infinitely long heat source. Though these hypotheses are not correct in the strict sense, they are sufficient for precise measurements of thermal properties. This method is achieved by measuring the response of temperature/time of the probe to a sudden electrical pulse. Thermometer and heater are both used by probe at the same time. A derivation of temperature data and Fourier's law are used to estimate the thermal conductivity.

Thermal conductivity is estimated by controller at the end of the reading by change the temperature (ΔT) with the time as

$$k = \frac{q''(\ln t_2 - \ln t_1)}{4\pi(\Delta T_2 - \Delta T_1)} \quad (5)$$

where ΔT_1 and ΔT_2 are the changes in the temperature at t_1 and t_2 times respectively, q'' is the applied constant heat rate to a small and an infinitely long (line) source.

2.2.1 Working of KD2 Pro

A 30 second equilibration time for each measurement cycle, 30 second for cool and a 30 second for heat time were used. Measurements of temperature are made during 1 second intervals for cooling and heating. These measurements are then fit with functions of exponential integral utilized a nonlinear least squares procedure. During the measurement, the temperature of the sample changes to correct a linear drift term, to optimize the precision of the readings. A microprocessor and a thermo-resistor are used to measure and control the conduction in the probe. Before measurement, for ensuring the thermal equilibrium between nanofluid sample and sensor needle, the temperature of the samples was kept fixed for 30 min by using the temperature-controlled container. Five separate measurements were repeated and the average value of thermal conductivity was taken. The experiments were considered only when a mean value of data has square correlation coefficient (R^2) value more than 0.9995 **KD2 pro user guide, 2014.**

Different techniques were tried to improve the KD2 Pro instrument accuracy during the measurements of thermal conductivity of nanofluid and are as follows:



- 1) The needle probe is taken out and cleaned after each measurement to avoid the agglomeration and sedimentation of nanoparticles of graphene upon it.
- 2) The sensor needle probe was immersed fully into the nanofluid, oriented vertically by fixing it through thick plastic cover for the container and centrally inside the container to avoid touching with walls side of the container. This vertical orientation of the needle probe insertion through the nanofluid will reduce the errors from free convection. Because a slight inclination of the needle from its vertical position will produce a large error.
- 3) Several other precautions were taken such as avoiding vibrations during measurement by placing the instrument on an optical table and switching off the chiller during the measurement. The KD2 pro instrument has been calibrated by measuring thermal conductivity of glycerol and DI-water at 20°C. The values of measuring glycerol and DI-water were 0.282 and 0.607 W/mK, which are in good agreement with the values from (**NIST, webbook**) of 0.285 and 0.598 W/mK, respectively, within $\pm 5\%$ accuracy.

3. RESULTS AND DISCUSSION

3.1 Results of Viscosity

Viscosity of fluids is one of the most significant parameters, which estimates the heat transfer fluid quality. In the absence of any prior data on the viscosity of GNPs based DI-water nanofluids in the literature, it is most significant to confirm whether they show Newtonian or non-Newtonian behavior as a function of both weight fraction concentrations and temperature of nanofluid.

3.1.1 Effect of Shear Strain on Viscosity

The viscosity of DI- water and GNPs based DI-water has been examined with various weight fractions (0.1–1wt %) and temperatures range of (5–35)°C. **Figs. 5 and 6** show the relationship between the viscosity and shear strain rate at temperature 5°C and 35°C, respectively. These figures show that the viscosity of the DI-water remains constant when the shear rate is increased. It is obviously that the DI-water displays a Newtonian behavior. Otherwise, the GNPs nanofluid displays Newtonian and Non-Newtonian behavior depends on the weight fraction concentration



and temperature. From figures the viscosity of the GNPs based DI-water nanofluid for a concentration (0.1wt%) decreases with increasing the shear strain rate and this refers to the GNPs nanofluid behave as non-Newtonian fluid until reaches specific value of shear strain (80 s^{-1}). After this value the viscosity remains constant when the shear strain increases. That indicates the nanofluid works as Newtonian fluids. However, it is clear that the shear thinning (non-Newtonian) behavior become more prominent with increasing the GNPs weight fraction concentration and decreasing the temperature of nanofluid.

The reason of this shear thinning (non-Newtonian) behavior of GNPs based DI-water nanofluid can be clarified commonly as follows. When the spindle rotates in the fluid, at low shear rates, the structure of molecules fluid changes gradually and temporarily align themselves with the increasing of shear rates direction. It generates less resistance and that causes a lowering in viscosity of nanofluid. The amount of shear ordering attained maximum, when the shear strain is high, and that causes to break down the aggregates to small sizes, hence the viscosity of nanofluid is decreasing **Alvarado, 2009**. If the shear rate increases more, it will not make unchanged on the viscosity. Because of large surface area and small size of the nanoparticles and there is a possibility for structuring at low shear strain rates and a restriction and deformation at high value of shear strain rates.

3.1.2 Effect of the Temperature on the Viscosity

Fig.7, shows reduction in the viscosity of the DI-water and GNPs nanofluid when the temperature is increasing. This due to that, when the temperature is rising, that causes the weakening of the adhesion forces for inter-particles intermolecular and that reduces the average forces of intermolecular. Subsequently, the viscosity reduces when the temperature increases. This is noticed for the most kinds of nanofluids **Elias, 2014**. **Figs. 8 and 9** show the maximum increment in viscosity of GNPs based DI-water is 111% at 1 wt% weight concentration and temperature $35 \text{ }^\circ\text{C}$ compared with base fluid.

The correlation is developed to calculate the viscosity of GNPs nanofluid depending on the experimental results with the limit of the temperature ($5\text{--}35^\circ\text{C}$) and weight fraction (0.1–1%) as shown in **Fig. 10**. It can be expressed as:

$$\mu_{nf} = (aT^2 + bT + c) \quad (6)$$



where a, b, and c are the fitting parameter as shown in **Table 1**.

Unfortunately, theoretical formulations to predict the temperature dependence of viscosity of GNPs nanofluids are practically absent **Ijam, 2015**.

3.1.3 Effect of Concentration on Nanofluid Viscosity

The viscosity of the GNPs based DI-water nanofluid is examined with various weight fraction concentrations, as shown in **Fig. 11**. It shows the viscosity of GNPs increment with increasing the weight fraction concentration. This is because the large surface area of the GNPs nanoparticles in contact and increasing the base fluid molecules resistance with increasing the weight fraction of GNPs nanoparticles.

The experimental data were compared with theoretical models that are proposed by other authors at 25°C temperature as shown in **Fig. 11**.

It can be seen from this figure that these theoretical models failed to calculate the viscosity of GNPs based water nanofluids. This may be due to variation in surface chemistry, morphology, shear rate and measurement technique, etc.

3.2 Results of Thermal Conductivity

Thermal conductivity of the GNPs nanofluids with various weight fraction concentrations and temperature ranging from (5 to 35°C) are shown in **Fig. 12**. It is clear from this figure that the thermal conductivity enhancement was obtained with increasing weight concentrations and temperature. **Fig. 13** shows the thermal conductivity enhancement ratio.

$$((k_{nf} - k_{bf}) / k_{bf}) \times 100 \quad (7)$$

where k_{bf} and k_{nf} were the thermal conductivities of base fluid and nanofluid, respectively.

The maximum enhancement ratio in thermal conductivity for 1 wt% of GNPs was 22% at 35 °C and 10% for 0.1 wt % concentration compared with base fluid.

The conventional theoretical models that have been developed to calculate nanofluids thermal conductivity, such as the Hamilton-Crosser model and the Maxwell model, considered only nanoparticles volume fraction and base fluid thermal conductivities, while particle shape, size, and motion and dispersed particles distribution do not show considerable effect on thermal



conductivity improvement. Hence, the results of the experiments cannot be compared with the values correlated by these traditional theoretical models. These models showed weakness in estimating the thermal conductivities of nanofluids which drove to suggest different new mechanisms. Many researchers **Choi, 2003, Kole, 2013, and Mehrali, 2014** indicated the Brownian motion of nanoparticles as an important factor for figure out the improvement. Recently, widely accepted idea leads the presence of nanolayer at liquid–solid interface and nanoparticles aggregation of may frame the prime contributing mechanisms for improvement of thermal conductivities in nanofluid. The liquid molecules close to nanoparticles surfaces forms layered structures and conduct as a solid.

GNPs have the largest surface area compared with spherical and nanotube shape of nanoparticles based nanofluids because it has two-dimensional structures. This mean that the GNPs will have considerable larger contact area/interface with the molecules of base fluid. Hence the resistance of contact (Kapitza resistance) will be reduced for the GNPs nanofluid interface considerably and that will assist to enhance the effective thermal conductivity of the GNPs nanofluid. This illustrates why the thermal conductivity of GNPs nanofluid is high.

Researchers from various organizations completed a benchmark research on the thermal conductivity of GNP nanofluids, and the data referred that the results of experiments were in better agreement with Nan's model. Accordingly to **Nan's model,1997**, the GNPs nanofluid thermal conductivity can be estimated as below:

$$k_{nf} = k_{bf} \frac{3 + \phi v [2\beta_{11}(1-L_{11}) + \beta_{33}(1-L_{33})]}{3 - \phi v (2\beta_{11}L_{11} + \beta_{33}L_{33})} \quad (8)$$

where ϕv and L_{ii} are the volume fraction and the geometrical factor of nanoparticles, respectively. β_{ii} is defined as

$$\beta_{ii} = \frac{k_p - k_{bf}}{k_{bf} - L_{ii}(k_p - k_{bf})}$$

where k_{bf} , k_p are the thermal conductivities of base fluid and nanoparticles respectively. The aspect ratio of GNPs is very high, therefore $L_{11} = 0$ and $L_{33} = 1$. Thermal conductivity estimated by Nan's model took into account the matrix additive interface contact resistance. The predicted thermal conductivity of composite in Eqs. (8), is very sensitive to the change in the nanoparticles



thermal conductivity of. Furthermore, the theoretical estimation confirmed that the graphene thermal conductivity of can be affected by the dimensions of nanoparticles, defect density and edge roughness. **Fig. 14** displays the thermal conductivity of GNPs nanofluid improvement at temperature of 30°C and as a function of weight fraction concentration. The results indicate that, data can be obtained by using Nan's model to predict thermal conductivity with a good accuracy.

The correlation is developed to estimate the GNPs based DI-water nanofluid thermal conductivity based on the experimental result with the limitation of the weight concentrations range of (0.1–1)% and temperature range of (5–35)°C as shown in **Fig. 15**. It can be expressed as the following equation:

$$k = (a T^2 + bT + c) \quad (9)$$

where a, b, and c are the fitting parameter as given in **Table 2**.

4. COMPARISON WITH PUBLISHED WORK

The comparison of the present experimental results of GNPs based DI-water nanofluid with the published work, of **Mehrali, 2014** and **Mehrali, 2015**, are shown in **Fig. 16** for thermal conductivity and **Fig. 17** for viscosity. These comparisons show a reasonable agreement with an error not exceeding 11%, 13% and respectively.

5. CONCLUSIONS

The thermophysical properties like thermal conductivity and viscosity of the suspensions of GNPs based DI-water nanofluid were examined for different weight fraction concentrations and temperatures. From this study it can be concluded that:

1. The thermal conductivity is increased with increasing the temperature of the GNPs nanofluid and nanoparticles weight concentrations, and maximum enhancement in thermal conductivity was around 11.9% to 22.2% with concentration of ($\phi_m=1\text{wt}\%$) and temperature range from 5 to 35°C.
2. The GNPs based DI-water nanofluid displayed a Newtonian and non-Newtonian behavior with respect to nanoparticles concentration and temperature. The viscosity of the nanofluid decreased with increasing the temperatures, and their increment was 80–111% compared with DI-water when the temperature increased from 5 to 35 °C.



3. The traditional models were not able to predict the viscosity and thermal conductivity of the GNPs based DI-water nanofluid. Therefore, correlations were suggested to evaluate the thermophysical properties based on the experimental results.

REFERENCE

- Brookfield Engineering Labs Inc., 2014," *Model DV-I PRIME Operating Instructions* "Manual No. M/07-022.
- Brookfield Engineering Labs, Inc., 2005, "*More Solutions to Sticky Problems*".
- Batchelor G.K., 1977,"*The effect of Brownian motion on the bulk stress in a suspension of spherical particles*", J. Fluid Mech. Vol.83, P.97–117.
- Brinkman H.C., 1952,"*The viscosity of concentrated suspensions and solutions*", J. Chem. Phys. Vol.20, P.571.
- Choi S., and Eastman A., 1995,"*Enhancing thermal conductivity of fluid with nanoparticles*", in: D.A. Siginer, *Developments and Applications of Non-Newtonian Flows*, Vol.66, PP.99–105.
- Dey T. K. and Kole M., 2013,"*Investigation of thermal conductivity, viscosity, and electrical conductivity of graphene based nanofluids*" Journal Of Applied Physics, Vol.113, PP.084307-1.
- Einstein A., 1956,"*Investigations on the Theory of the Brownian Movement*", Courier Dover Publications.
- Elias M., Mahbulul I., Saidur R. and Sohel M., 2014,"*Experimental investigation on the thermophysical properties of Al₂O₃ nanoparticles suspended in car radiator coolant*" International communications in Heat Mass Transfer Vol.54, PP.48–53.
- Ijam A., Saidur R., Ganesan P. and Golsheikh A., 2015,"*Stability, thermo-physical properties, and electrical conductivity of graphene oxide deionized water/ethylene glycol based nanofluid*", International Journal of Heat and Mass Transfer, Vol.87, PP.92–103.
- Murshed S.M.S, and Yang C., 2008,"*Thermophysical and electrokinetic properties of nanofluids*" – A critical review, Vol.28, PP.2109-2125.
- Mehrali M., Sadeghinezhad E., Latibari S., Kazil S., 2014,"*Investigation of thermal conductivity and rheological properties of nanofluids containing graphene nanoplatelets*", Nanoscale Research Letters, 9:15.
- Mehrali M., Sadeghinezhad E. and Rosenc A., 2015, "*Heat transfer and entropy generation for laminar forced convection flow of graphene nanoplatelets nanofluids in a horizontal tube*", International Communications in Heat and Mass Transfer Vol.66, PP.23–31.
- National institute of standards and technology (NIST), 2015. <http://webbook.nist.gov/chemistry/fluid>



- Nan Ce-Wen and Birringer R., 1997,"*Effective thermal conductivity of particulate composites with interfacial thermal resistance*", Journal of Applied Physics, Vol.81 PP.6692-6699.
- Novoselov K., Geim A., Morozov S., Dubonos S. and Firsov A., 2004,"*Electric field effect in atomically thin carbon films*", Science Vol.306, PP. 666.
- Ramaprabhu S.and Baby T., 2010,"*Investigation of thermal and electrical conductivity of graphene based nanofluids*", Journal of Applied Physics Vol.108, PP.124308.
- Rashidi A., M.Ghozatloo A. and Shariaty-Niasar M., 2013,"*Preparation of nanofluids from functionalized Graphene by new alkaline method and study on the thermal conductivity and stability*" International Communications in Heat and Mass Transfer Vol.42, PP.89–94.
- Rashidi A., Hajjar Z., and Ghozatloo A., 2014,"*Enhanced thermal conductivities of graphene oxide nanofluids*" International Communications in Heat and Mass Transfer Vol.57, PP.128–131.
- Wang X., Xu X. and Choi S., 1999,"*Thermal conductivity of nanoparticle-fluid mixture*", J. Thermophys. Heat Transfer Vol.13, P.474–480.
- Yu W., Xie H., Wang X., Wang X.,2011,"*Significant thermal conductivity enhancement for nanofluids containing graphene nanosheets*", Physics Letters A Vol.375, PP.1323-1328.

NOMENCLATURE

AFG alkaline functionalized Graphene

EG ethylene glycol

f-HEG fictionalized graphene

GO graphene oxide

GNPs single layer Graphene

NIST National Institute of Standards and Technology

γ =shear strain, N/m^2 .

μ_{bf} =dynamic viscosity of base fluid, kg/m.s.

τ =shear stress, N/m^2 .

ω =angular speed of the spindle

M=torque input by the viscometer, N/m^2 .

R_c =radius of the sample container, m

μ =dynamic viscosity, kg/m.s.

R_{sp} =radius of the spindle, m

μ_{nf} =dynamic viscosity of nanofluid, kg/m.s.

N=rotational speed of the spindle



L =effective length of the spindle,m

k =Thermal conductivity, W/m.K

k_p =Thermal conductivity of particle, W/m.K

k_{bf} =Thermal conductivity of base fluid, W/m.K

k_{nf} =Thermal conductivity of nanofluid, W/m.K

q'' = heat flux,W/m²

T =temperature, °C.

t =time, second.

L_{ii} =geometrical factor, dimensionless

ϕ_v =particle volume faction, dimensionless

ϕ_m =mass fraction of the particles, dimensionless

ρ_p =density of the nanoparticle, kg/m³.

ρ_b =density of base fluid, kg/m³.

Table 1. Values of factors for viscosity of GNPs nanofluid.

ϕ_m	a	b	c	R ²
0 wt%	0.00052	-0.04695	1.73063	0.9993
1 wt%	0.00047	-0.05921	3.01429	0.9977
0.9 wt%	0.00052	-0.05995	2.88714	0.9988
0.8 wt%	0.00059	-0.06348	2.79571	0.9993
0.7 wt%	0.00066	-0.0654	2.70429	0.9989
0.6 wt%	0.00086	-0.07298	2.65571	0.9978
0.5 wt%	0.00083	-0.06683	2.41857	0.9982
0.4 wt%	0.00045	-0.0479	2.14429	0.9989
0.3 wt%	0.0005	-0.04795	2.02857	0.9992
0.2 wt%	0.00047	-0.0462	1.93071	0.9989
0.1 wt%	0.0062	-0.05048	1.87143	0.9973

Table 2. Values of factors for thermal conductivity of GNPs nanofluid.

ϕ_m	a	b	c	R ²
0 wt%	0.00001	0.001757	0.5628	0.9985
1 wt%	0.00006	0.00173	0.6294	0.9983
0.8 wt%	0.00005	0.00177	0.6198	0.9964
0.6 wt%	0.00005	0.00145	0.6168	0.9901
0.4 wt%	0.00005	0.00106	0.6151	0.9812
0.2 wt%	0.00007	0.00022	0.614	0.995
0.1 wt%	0.00005	0.000829	0.592	0.9939



Figure 1. Brookfield DV-I Prime Viscometer.

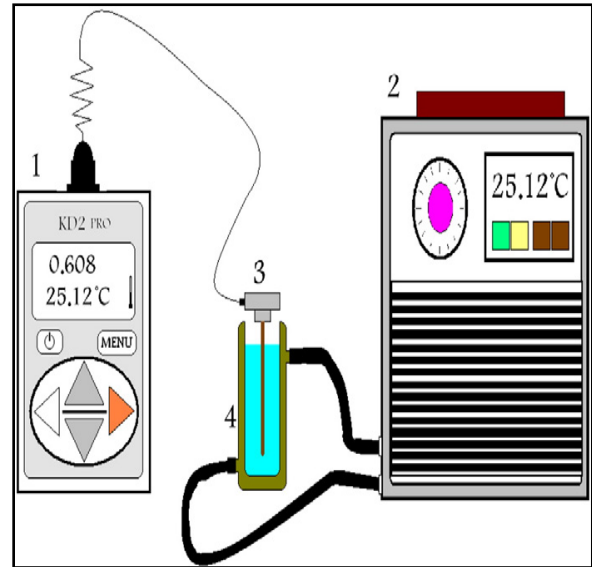


Figure 2. Scheme of experimental set-up to measure thermal conductivity.

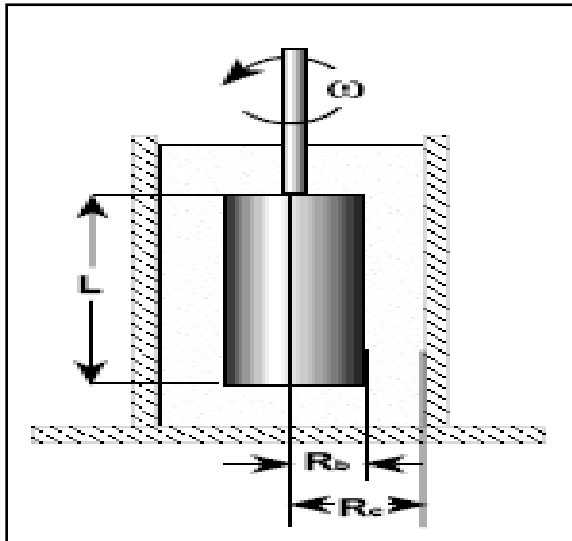


Figure 3. Diagram to explain the dimension parameters.

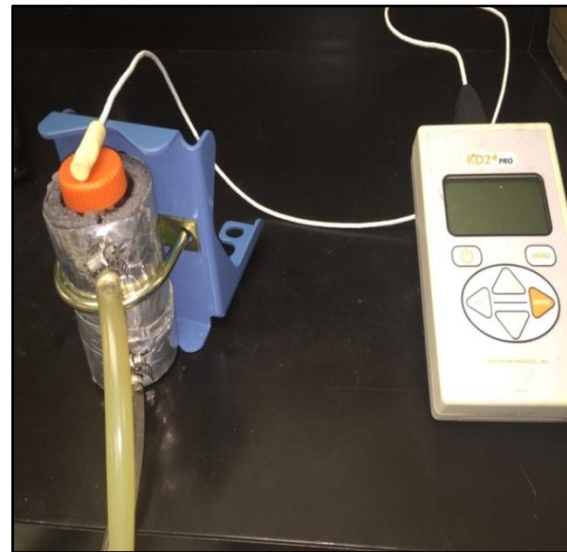


Figure 4. Set-up of experiment to measure thermal conductivity.

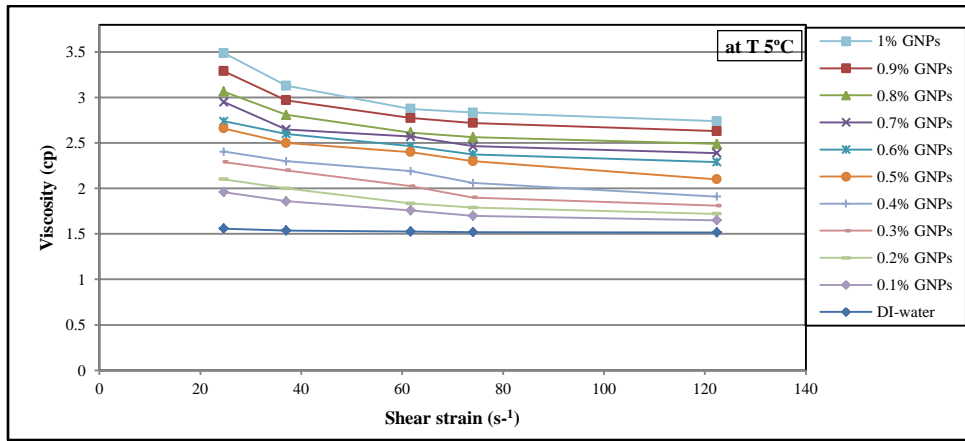


Figure 5. Effect of shear rate on viscosity of GNPs nanofluid with different weight concentrations.

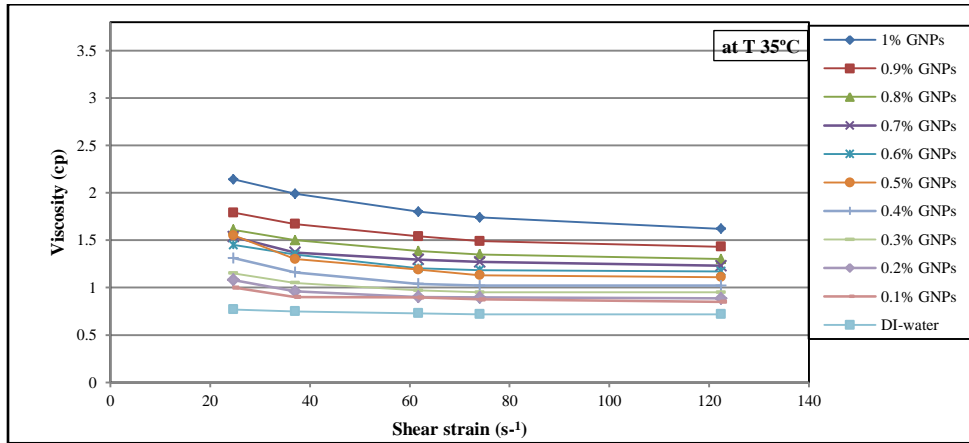


Figure 6. Effect of shear rate on viscosity of GNPs nanofluid with different weight concentrations.

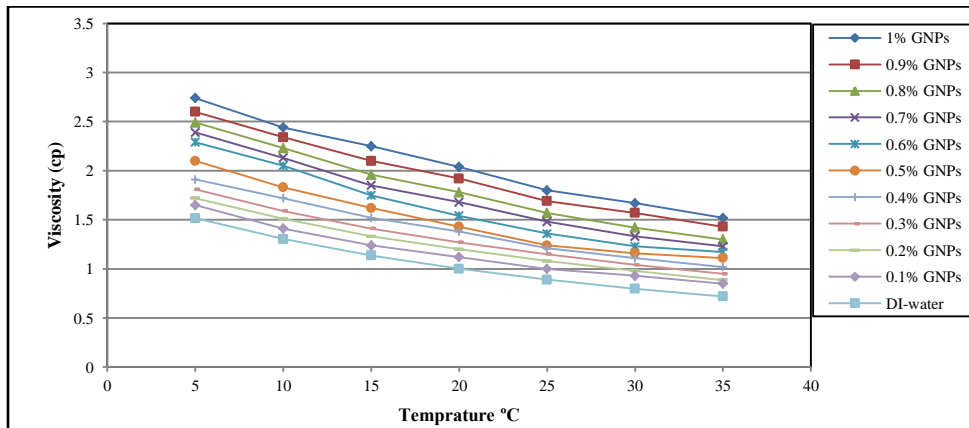


Figure 7. Effect of temperature on viscosity of GNPs nanofluid with different weight concentrations.

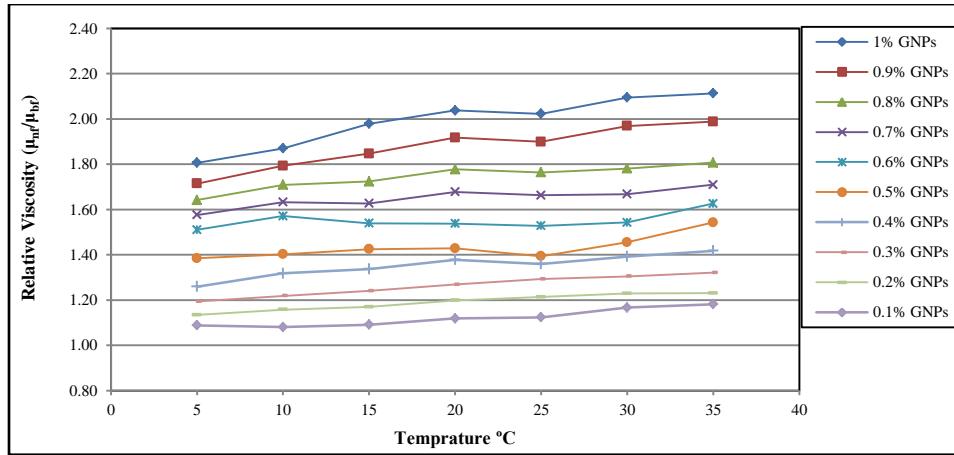


Figure 8. Effect of temperature on relative viscosity of GNPs nanofluid with different weight concentrations.

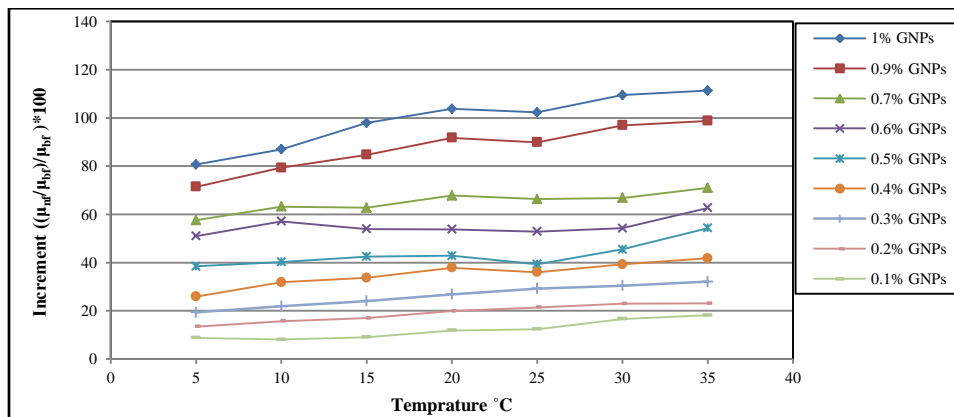


Figure 9. Effect temperature on increment of viscosity of GNPs nanofluid at different concentrations.

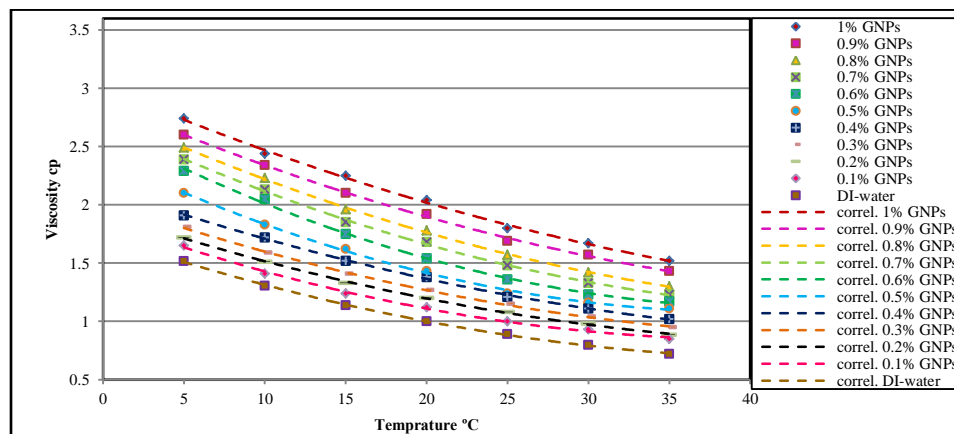


Figure 10. Correlation of experimental results of viscosity for GNPs nanofluid at different temperatures and concentrations.

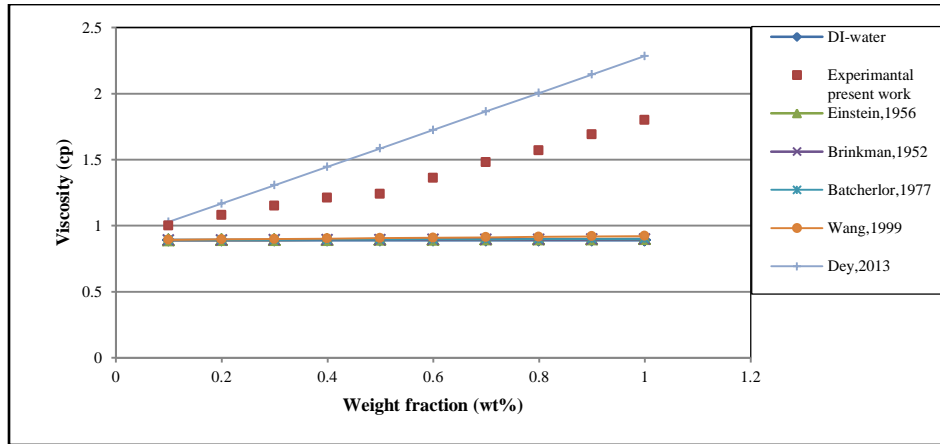


Figure 11. Effect of weight fraction concentration on viscosity of GNPs nanofluid at (35°C) with other references.

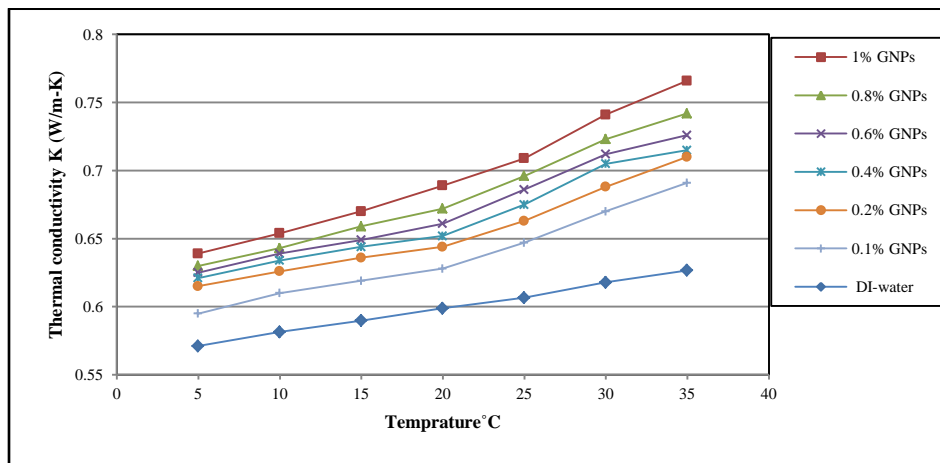


Figure 12. Effect of temperature on thermal conductivity of GNPs with different weight concentrations.

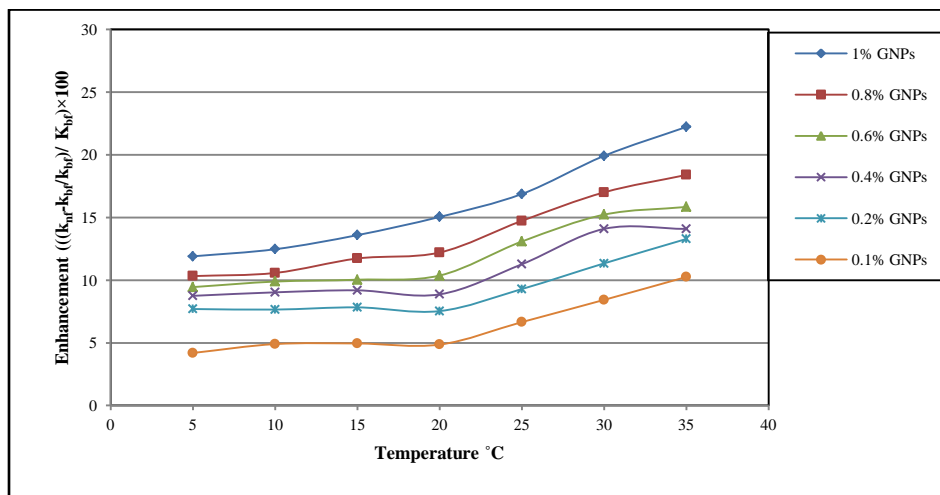


Figure 13. Effect of temperature on thermal conductivity enhancement percentage compared with DI-water.

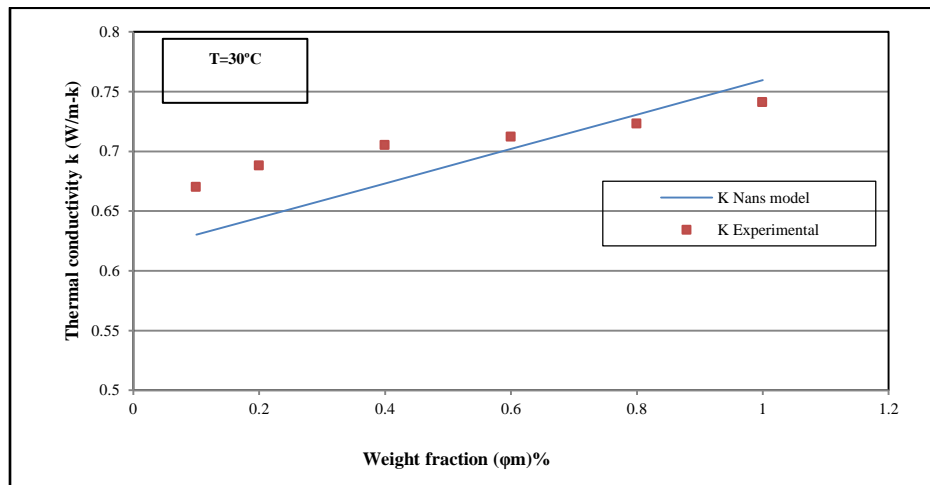
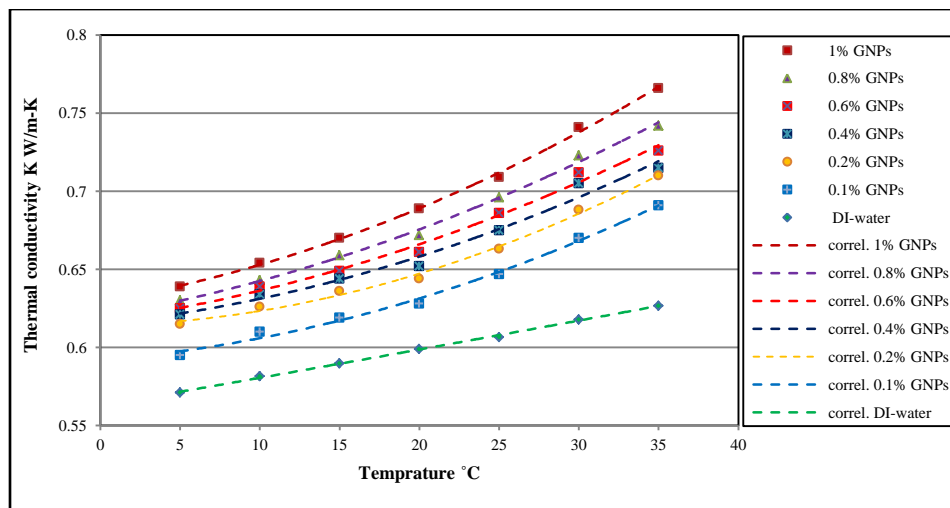


Figure 14. Comparison of experimental thermal conductivity results of GNPs nanofluid with Nan's model.



Figures 15. Correlation of experimental results of thermal conductivity for GNPs nanofluid at different temperatures and concentrations.

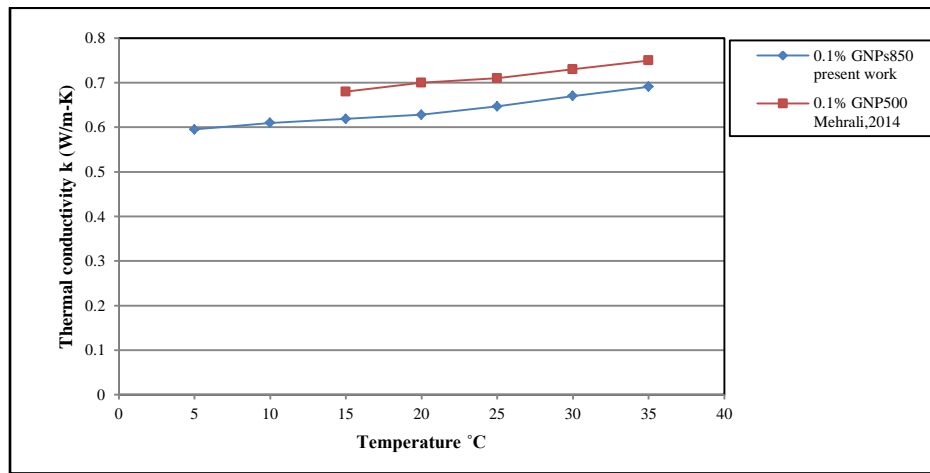


Figure 16. Comparison of experimental results of thermal conductivity for present work with the published data of **Mehrali, 2014.**

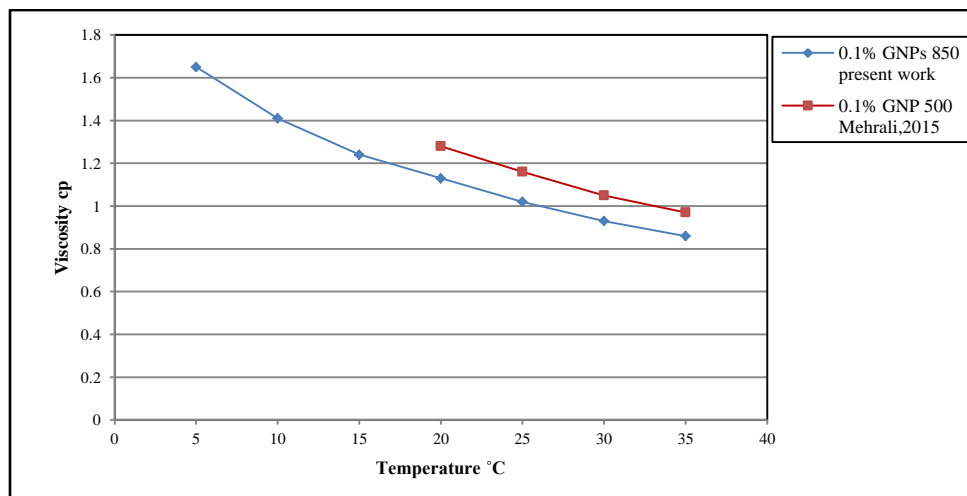


Figure 17. Comparison of experimental results of viscosity for present work with the published data of **Mehrali, 2014.**